Supplement of Biogeosciences, 15, 3561–3576, 2018
https://doi.org/10.5194/bg-15-3561-2018-supplement

Supplement of

Seasonal patterns in phytoplankton biomass across the northern and deep Gulf of Mexico: a numerical model study

Fabian A. Gomez et al.

Correspondence to: Fabian A. Gomez (fabian.gomez@noaa.gov)

S1. Biogeochemical Model Equation and Parameters

Variables:

NH_4: Ammonium

NO_3: Nitrate

PS: Phytoplankton small (nanophytoplankton)

PL: Phytoplankton large (diatom)

ZS: Zooplankton small (microzooplankton)

ZL: Zooplankton large (mesozooplankton)

DS: Small detritus (slow sinking detritus)

DL: Fast detritus (fast sinking detritus)

DON: Dissolved organic nitrogen

$SiOH_4$: Silicate

Opal: Particulate silica

CHL_S: Chlorophyll PS

CHL_L: Chlorophyll PL

I: Photosynthetic Available Radiation

T: Temperature

Processes:

μ_{NO3}: phytoplankton growth fuelled by NO_3

μ_{NH4}: phytoplankton growth fuelled by NH_4

exud: phytoplankton exudation

$graz_{ps}$: zooplankton grazing upon PS

$graz_{pl}$: zooplankton grazing upon PL

pred: ZL predation upon ZS

excr: zooplankton excretion

egest: zooplankton egestion

mort: mortality

decomp: decomposition of organic nitrogen and opal

nitr: nitrification

$uptake_{Si}$: PL uptake of SiOH4

μ_{CHL}: chlorophyll production

$graz_{CHL}$: chlorophyll loss due to zooplankton grazing

$mort_{CHL}$: chlorophyll loss due to phytoplankton mortality

Dynamic equations

$$\frac{\delta PS}{\delta t} = \mu_{NO3}(PS) + \mu_{NH4}(PS) - graz_{ps}(ZS) - graz_{ps}(ZL) - mort(PS) - exud(PS)$$

$$\frac{\delta PL}{\delta t} = \mu_{NO3}(PL) + \mu_{NH4}(PL) - graz_{pl}(ZS) - graz_{pl}(ZL) - mort(PL) - exud(PL) - w_p \frac{\delta PL}{\delta z}$$

$$\frac{\delta ZS}{\delta t} = graz_{ps}(ZS) + graz_{pl}(ZS) - pred(ZL) - mort(ZS) - excr(ZS) - eges(ZS)$$

$$\frac{\delta ZL}{\delta t} = graz_{ps}(ZL) + graz_{pl}(ZL) + pred(ZL) - mort(ZL) - excr(ZL) - eges(ZL)$$

$$\frac{\delta DS}{\delta t} = mort(PS) + mort(ZS) + egest(ZS) - decomp_{NH4}(DS) - decomp_{DON}(DS) - w_{DS} \frac{\delta DS}{\delta z}$$

$$\frac{\delta DL}{\delta t} = mort(PL) + mort(ZL) + egest(ZL) - decomp_{NH4}(DL) - decomp_{DON}(DL) - w_{DL} \frac{\delta DL}{\delta z}$$

$$\frac{\delta NO_3}{\delta t} = -\mu_{NO3}(PS) - \mu_{NO3}(PL) + nitr$$

$$\frac{\delta NH_4}{\delta t} = -\mu_{NH4}(PS) - \mu_{NH4}(PL) + decomp_{NH4}(DS) + decomp_{NH4}(DL) + decomp_{NH4}(DON)$$

$$\frac{\delta DON}{\delta t} = exud(PS) + exud(PL) + decomp_{DON}(DS) - decomp_{DON}(DL) - decomp_{NH4}(DON)$$

$$\frac{\delta Si(OH)_4}{\delta t} = -uptake_{Si}(PL) + exud_{Si}(PL) + decomp_{Si}(Opal\ )$$

$$\frac{\delta opal}{\delta t} = mort_{Si}(PL, ZL) + egest_{Si}(ZS, ZL) - decomp_{Si}(Opal\ ) - w_{opal} \frac{\delta opal}{\delta z}$$

$$\frac{\delta CHL_S}{\delta t} = \mu_{CHL_S} - graz_{CHL_S}(ZS, ZL) - mort_{CHL_S}$$

$$\frac{\delta CHL_L}{\delta t} = \mu_{CHL_L} - graz_{CHL_L}(ZS, ZL) - mort_{CHL_L} - w_p \frac{\delta CHL_L}{\delta z}$$

Processes equations

1. Growth Phytoplankton Small

1.1 $\mu_{NO3}(PS) = V_S \cdot \left(\frac{NO_3}{K_{NO3S}+NO_3}\right)\left(\frac{1}{1+NH_4/K_{NH4S}}\right) \cdot PS$

1.2 $\mu_{NH4}(PS) = V_S \cdot \left(\frac{NH_4}{K_{NH4S}+NH_4}\right) \cdot PS$

1.3 $V_S = V_{pS} \cdot f_{PS}(I)$

1.4 $V_{pS} = V_{maxS} \cdot e^{k_{Gpp} \cdot T}$

1.5 $NL_{PS} = \left(\frac{NO_3}{K_{NO3S}+NO_3}\right)\left(\frac{1}{1+NH_4/K_{NH4S}}\right) + \left(\frac{NH_4}{K_{NH4S}+NH_4}\right)$

1.6 $f_{PS}(I) = \frac{\alpha_{PS} I}{\sqrt{(\alpha_{PS} I)^2 + V_{pS}^2}}$

2. Growth Phytoplankton Large

2.1 $\mu_{NO3}(PL) = V_L \left(\frac{NO_3}{K_{NO3L}+NO_3}\right) \cdot \left(\frac{1}{1+NH_4/K_{NH4L}}\right) \cdot min\left\{1, \left(\frac{L_{Si}}{L_N}\right)\right\} \cdot PL$

2.2 $\mu_{NH4}(PL) = V_L \left(\frac{NH_4}{K_{NH4L}+NH_4}\right) \cdot min\left\{1, \left(\frac{L_{Si}}{L_N}\right)\right\} \cdot PL$

2.3 $V_{pL} = V_{maxL} \cdot e^{k_{Gpp} \cdot T}$

2.4 $V_L = V_{pL} \cdot f_{PL}(I)$

2.5 $NLF = \left(\frac{NO_3}{K_{NO3L}+NO_3}\right) \cdot \left(\frac{1}{1+\frac{NH_4}{K_{NH4L}}}\right) + \left(\frac{NH_4}{K_{NH4L}+NH_4}\right)$

2.6 $SLM = \left(\frac{SiOH_4}{K_{Si}+SiOH_4}\right)$

2.7 $NL_{PL} = min\{NLF, SLF\}$

2.8 $f_{PL}(I) = \frac{\alpha_{PL} I}{\sqrt{(\alpha_{PL} I)^2 + V_{pL}^2}}$

3. Phytoplankton Exudation

3.1 $exud(PS) = \varphi_{PS} \cdot \left(\mu_{NH4}(PS) + \mu_{NO3}(PS)\right)$

3.2 $exud(PL) = \varphi_{PL} \cdot \left(\mu_{NH4}(PL) + \mu_{NO3}(PL)\right)$

4. Grazing Zooplankton Small

4.1 $graz_{PS}(ZS) = GR_{mPZS} \cdot e^{k_{ZMor} \cdot T} \left(\frac{PS^2}{PS^2 + K_{PSZS}}\right) \cdot ZS$

4.2 $graz_{PL}(ZL) = GR_{mPLZS} \cdot e^{k_{ZMor} \cdot T} \left(\frac{PL^2}{PL^2 + K_{PLZS}}\right) \cdot ZS$

5. Grazing-Predation Zooplankton Large

5.1 $graz_{PS}(ZL) = GR_{mPSZ} \cdot e^{k_{ZMor} \cdot T} \left(\frac{PS^2}{PS^2 + K_{PSZL}}\right) \cdot ZL$

5.2 $graz_{PL}(ZL) = GR_{mPLZL} \cdot e^{k_{ZMor} \cdot T} \left(\frac{PL^2}{PL^2 + K_{PLZL}}\right) \cdot ZL$

5.3 $pred_{ZS}(ZL) = GR_{mZSZL} \cdot e^{k_{ZMor} \cdot T} \left(\frac{ZS^2}{ZS^2 + K_{ZSZL}}\right) \cdot ZL$

6. Zooplankton Egestion

6.1 $egest(ZS) = (1 - \alpha_{ZS}) \cdot \left(graz_{PS}(ZS) + graz_{PL}(ZS)\right)$

6.2 $egest(ZL) = (1 - \alpha_{ZL}) \cdot \left(graz_{PS}(ZL) + graz_{PL}(ZL) + pred_{ZS}(ZL)\right)$

7. Zooplankton Excretion

7.1 $excr(ZS) = (\alpha_{ZS} - \beta_{ZS}) \cdot \left(graz_{PS}(ZS) + graz_{PL}(ZS)\right)$

7.2 $excr(ZL) = (\alpha_{ZS} - \beta_{ZS}) \cdot \left(graz_{PS}(ZL) + graz_{PL}(ZL) + pred_{ZS}(ZL)\right)$

8. Plankton Mortality

8.1 $mort(PS) = PMor_S \cdot e^{k_{PMor} \cdot T} \cdot PS$

8.2 $mort(PL) = PMor_L \cdot e^{k_{PMor} \cdot T} \cdot PL$

8.3 $mort(ZS) = ZMor_S \cdot e^{k_{ZMor} \cdot T} \cdot ZL$

8.4 $mort(ZL) = ZMor_L \cdot e^{k_{ZMor} \cdot T} \cdot ZL$

9. Decomposition/Remineralization

9.1 $decomp_{NH4}(DS) = \tau_{NH4_S} \cdot e^{k_D \cdot T} \cdot DS$

9.2 $decomp_{NH4}(DL) = \tau_{NH4_L} \cdot e^{k_D \cdot T} \cdot DL$

9.3 $decomp_{DON}(DS) = \tau_{DON_S} \cdot e^{k_D \cdot T} \cdot DS$

9.4 $decom_{DON}(DL) = \tau_{DON_L} \cdot e^{k_D \cdot T} \cdot DL$

9.5 $decomp_{NH4}(DON) = \gamma_{NH4} \cdot e^{k_D \cdot T} \cdot DON$

9.6 $nitr = Nit \cdot e^{k_{Nit} \cdot T} \cdot \left(1 - \frac{I - I_{th}}{D_p + I - 2 \cdot I_{th}}\right) \cdot NH_4$

10. Silica

10.1 $uptake_{Si}(PL) = (\mu_{NH4}(PL) + \mu_{NH4}(PL)) \cdot Si{:}N$

10.2 $exud_{Si}(PL) = exud_{DON}(PL) \cdot Si{:}N$

10.3 $decom_{Si}(opal) = \tau_{Si} \cdot e^{k_{Si} \cdot T} \cdot opal$

10.4 $mort_{Si}(PL, ZL) = \big(mort(PL) + mort(PL)\big) \cdot Si{:}N$

10.5 $egest_{Si}(ZS, ZL) = \big((1 - \alpha_{ZS}) \cdot graz_{PL}(ZS) + (1 - \alpha_{ZL}) \cdot graz_{PL}(ZL)\big) \cdot Si{:}N$

11. Chlorophyll Phytoplankton Small

11.1 $\mu_{CHL_S} = \big(\mu_{NH4}(PS) + \mu_{NO3}(PS)\big) \cdot \rho_{CHL_S} \cdot CHL_S$

11.2 $\rho_{CHL_S} = \frac{\theta_{maxS} \cdot \mu_S \cdot PS}{\alpha_{PS} \cdot I \cdot CHL_S}$

11.3 $graz_{CHL_S}(ZS, ZL) = (graz_{PS}(ZS) + graz_{PS}(ZL)) \left(\frac{CHL_S}{PS}\right)$

11.4 $mort_{CHL_S} = PMor_s \cdot e^{k_{PMor} \cdot T} \cdot CHL_S$

12. Chlorophyll Phytoplankton Large

12.1 $\mu_{CHL_L} = \big(\mu_{NH4}(PL) + \mu_{NO3}(PL)\big) \cdot \rho_{CHL_L} \cdot CHL_L$

12.2 $\rho_{CHL_L} = \frac{\theta_{maxL} \cdot \mu_L \cdot PL}{\alpha_{PL} \cdot I \cdot CHL_L}$

12.3 $graz_{CHL_L}(ZS, ZL) = (graz_{PL}(ZS) + graz_{PL}(ZL)) \left(\frac{CHL_L}{PL}\right)$

12.4 $mort_{CHL_L} = PMor_L \cdot e^{k_{PMor} \cdot T} \cdot CHL_L$

13. Light attenuation

13.1 $I_z = I_0 \cdot e^{Att \cdot z}$

13.2 $Att = Att_{sw} + Att_{PS} \cdot CHL_S + Att_{PL} \cdot CHL_L$

Sediment flux formulation

$$\frac{\delta NH_4}{\delta t} = \left[(w_P PL + w_{DS} DS + w_{DL} DL) \cdot \frac{4}{16\Delta z}\right]_{z=H}$$

$$\frac{\delta SiOH_4}{\delta t} = \left[\frac{(w_{Si} \cdot opal)}{\Delta z} \cdot 0.9\right]_{z=H}$$

S2. Model-Data Comparison of Physical Variables

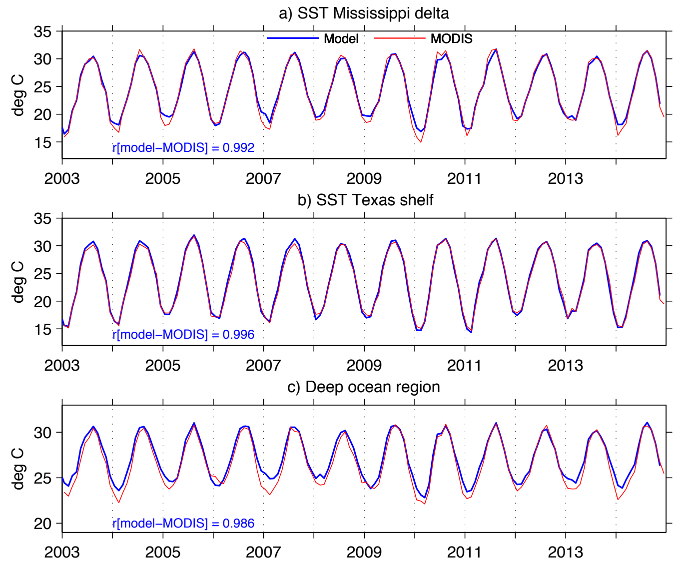

Figure S1. Monthly time series of SST derived from model outputs and MODIS for the Mississippi delta, Texas shelf, and Deep Gulf regions. Correlation coefficient between model and MODIS series are indicated at each panel. Monthly mean composite fields of MODIS SST (2003-2014) were retrieved from the Institute for Marine and Remote Sensing, University of South Florida (http://imars.usf.edu).

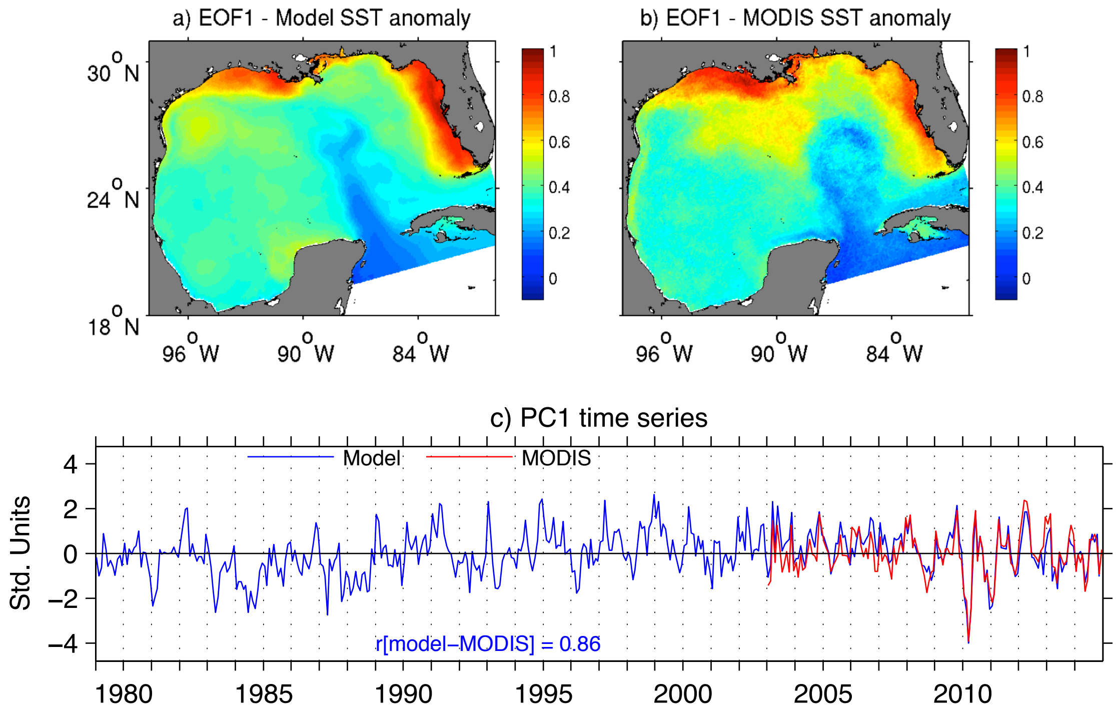

Figure S2. a-b) First Empirical Orthogonal Function (EOF1) of model and MODIS SST anomalies (seasonal cycle removed). c) First Principal Component time series (PC1) of model and MODIS SST anomalies. Correlation coefficient between model and MODIS PC1 is indicated in panel c. Monthly mean composite fields of MODIS SST (2003-2014) were retrieved from the Institute for Marine and Remote Sensing, University of South Florida (http://imars.usf.edu).

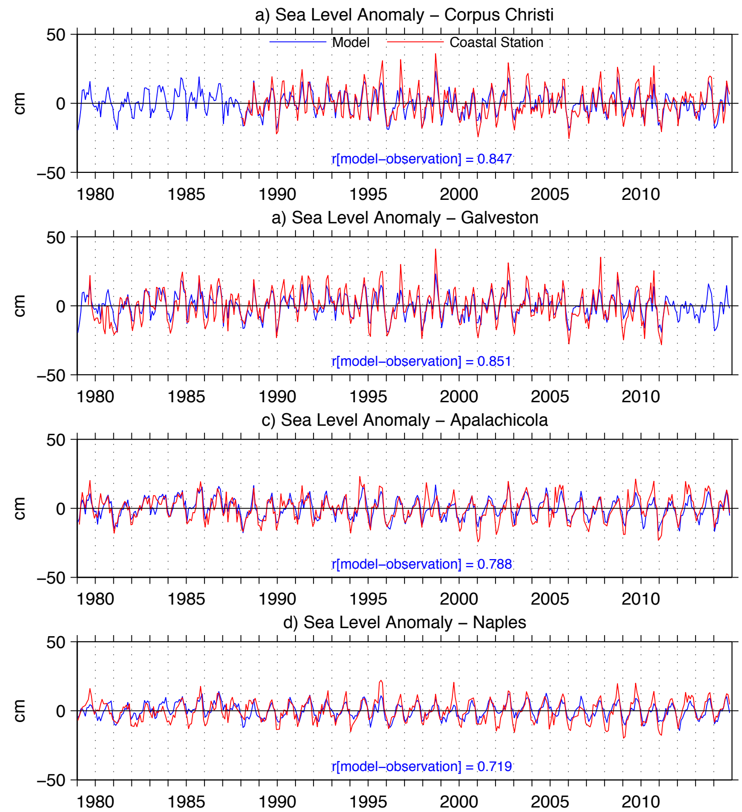

Figure S3. Monthly sea level anomaly derived from model (blue) and coastal observations (red) at a) Corpus Christi (27° 35'N, 97°13'W), b) Galveston (29° 17'N, 94° 47'W), c) Apalachicola (29° 43'N, 84° 58'W), and d) Naples (26° 7'N, 81° 48'W). Correlation (r) between modelled and observed time series is indicated at each panel. Coastal sea level observations were retrieved from the Sea Level Center, University of Hawaii (https://uhslc.soest.hawaii.edu).

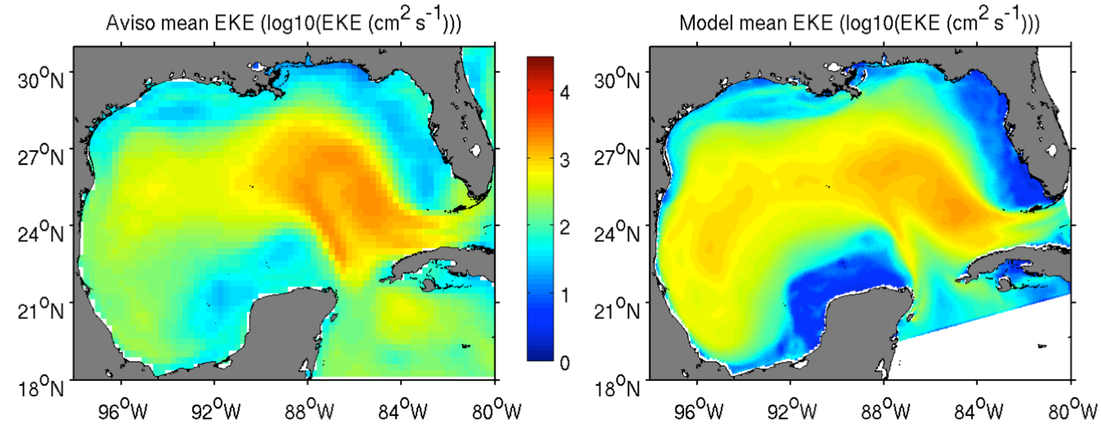

Figure S4. Mean Eddy Kinetic Energy (EKE) derived from AVISO sea surface height (left) and model (right) during period 1993-2010. Sea level anomalies used to estimate observed EKE were derived from Ssalto/Duacs altimeter products produced and distributed by the Copernicus Marine and Environment Monitoring Service (CMEMS) (http://www.marine.copernicus.eu).

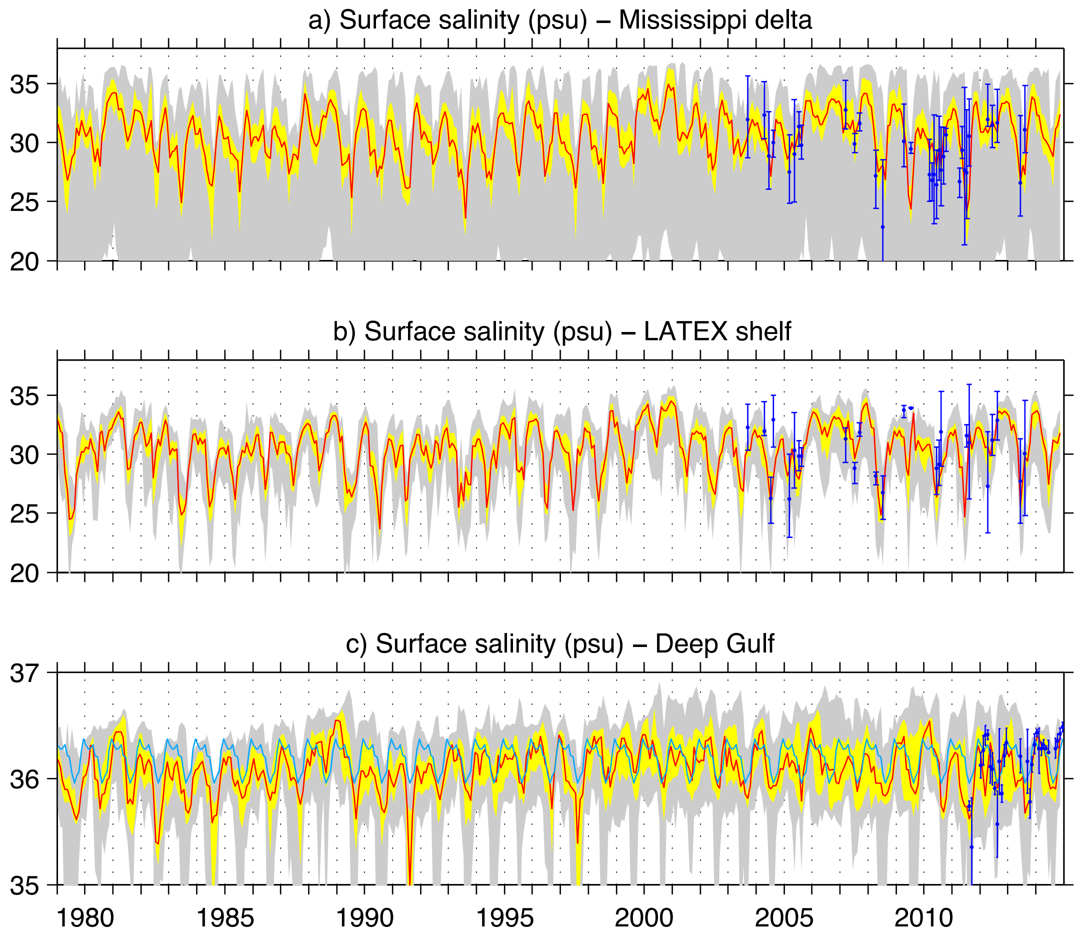

Figure S5. Surface salinity time series in the Mississippi delta, Texas shelf, and Deep Ocean region (regions are depicted in Fig. 1) The red line and grey area represent the mean and range model salinity, respectively, while in situ observations are in blue. Light blue line in panel c is the climatological salinity pattern derived from observations. Salinity data from the Mississippi delta and LATEX shelf were derived from CTD cast and Niskin bottle samplings collected during research cruises from the Louisiana Universities Marine Consortium (available at the Gulf of Mexico Coastal Ocean Observing System, http://data.gcoos.org) and the Gulf of Mexico Research Initiative (http://gulfresearchinitiative.org). Salinity data from the Deep Ocean were derived from APEX profiling floats from the Lagrangian Approach to Study the Gulf of Mexico Deep Circulation project 2011-07 to 2015-06 (https://data.nodc.noaa.gov).

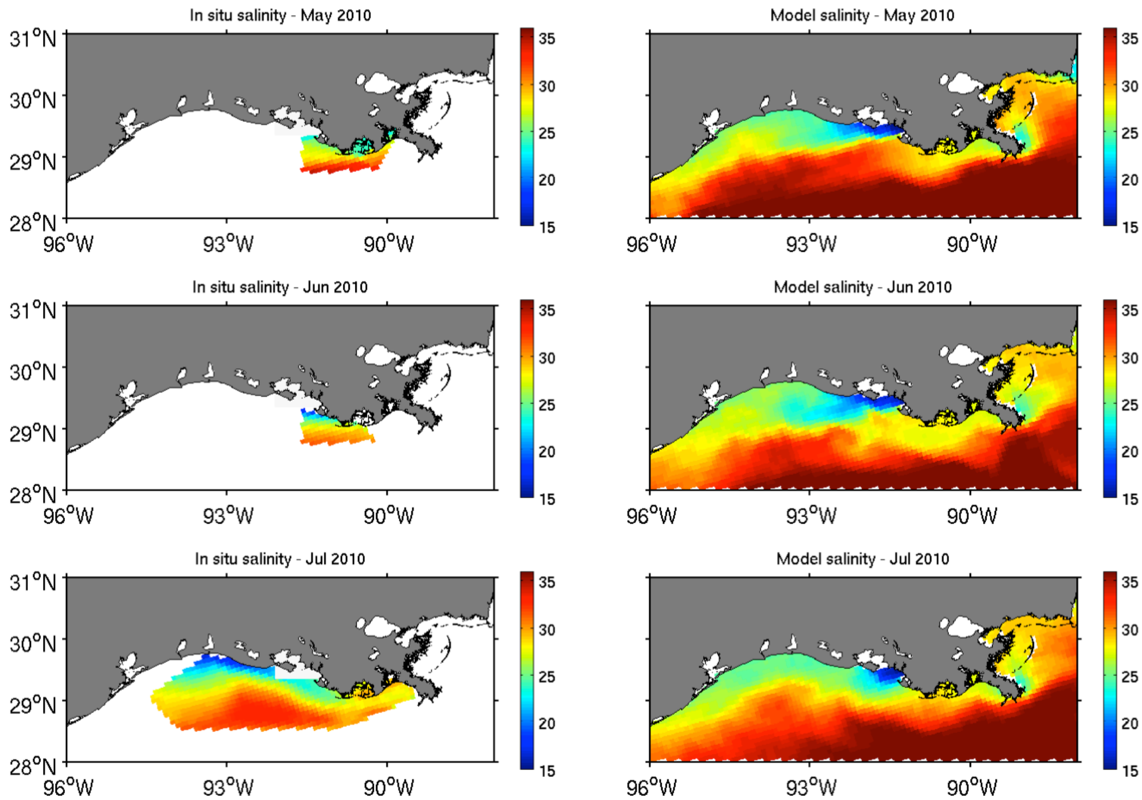

Figure S6: Comparison between in situ (left) and modelled (right) surface salinity during May-July of 2010. In situ observations are from the Louisiana Universities Marine Consortium, available in the Gulf of Mexico Research Initiative (http://gulfresearchinitiative.org).

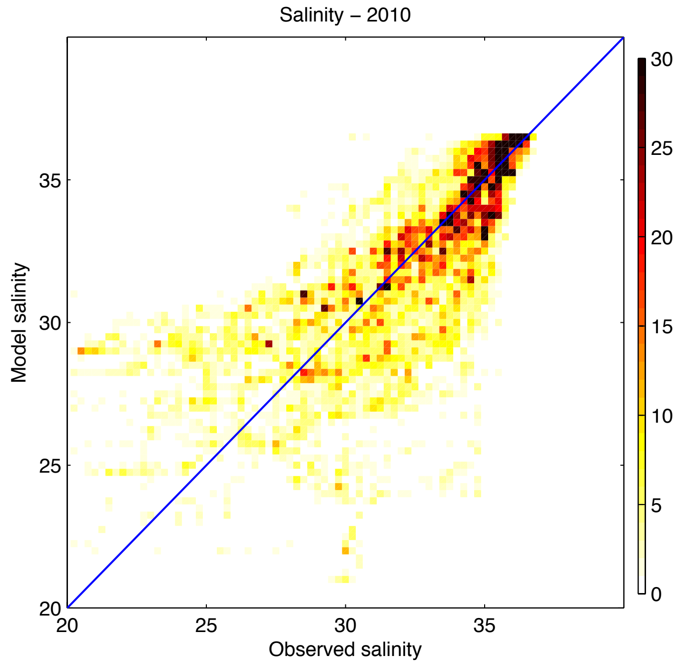

Figure S7: Comparison between in situ and model salinity over the Louisiana-Texas shelf during 2010. Relationship is shown as a 2-dimensional histogram (see color-scale). In situ observations are from the Louisiana Universities Marine Consortium, available in the Gulf of Mexico Research Initiative (http://gulfresearchinitiative.org).

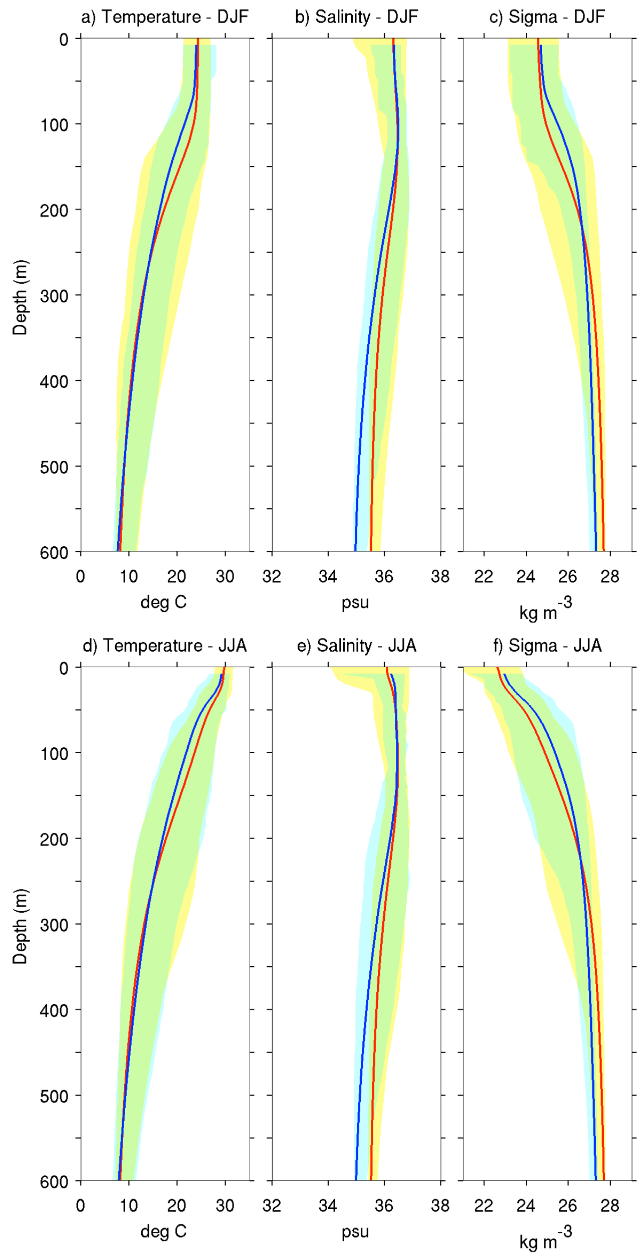

Figure S8: Climatological vertical profiles of temperature, salinity, and density for winter (a-c) and summer (d-f) derived from model outputs and APEX profiling floats during 2011-2014 in the Deep Gulf. Red (blue) lines and yellow (cyan) shadows represent the model (observed) mean and range, respectively. APEX data were collected in the Lagrangian Approach to Study the Gulf of Mexico Deep Circulation project 2011-07 to 2015-06 (available at https://data.nodc.noaa.gov).

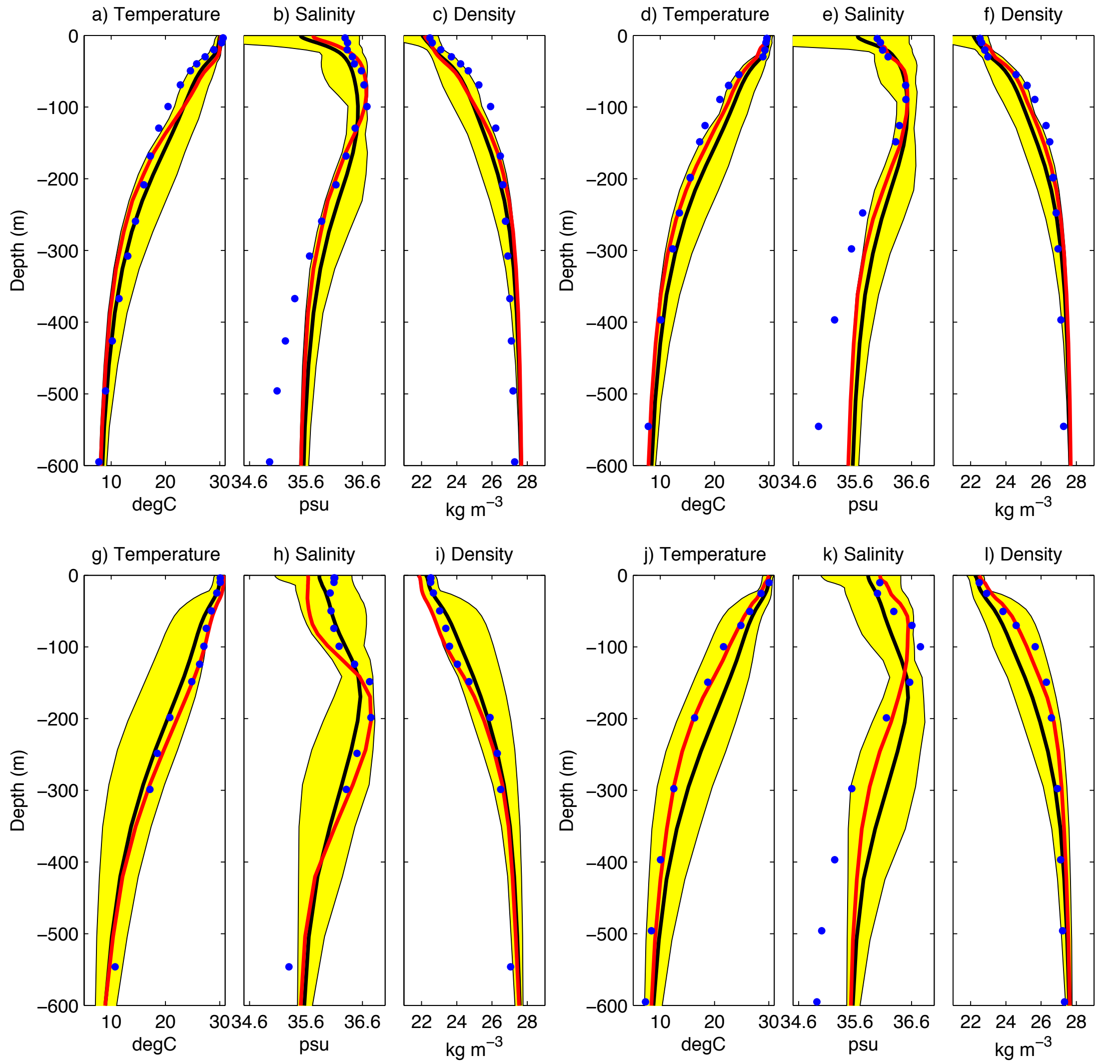

Figure S9: Comparison between profiles of temperature, salinity, and density derived from model outputs (red lines) and GOMMEC data (blue dots) at four-selected GOMMEC stations during July of 2007 (a-c, g-i) and July of 2012 (d-f, j-l). In addition, the model's climatological mean and range for July are shown as black line and yellow area, respectively. a-c) Station-18 GOMMEC-1 (90°W, 27.6°N); d-f) Station-1 GOMMEC-2 (90°W, 27.6°N); d-f); Station-28 GOMMEC-1 (86.4°W, 25.8°N); Station-12 GOMMEC-2 (86°W, 26°N). GOMMEC cruise data was obtained from CTD-cast measurements (available at http://www.aoml.noaa.gov). Profiles in upper and lower panels are derived from the most oceanic stations within the Mississippi and Tampa lines, respectively (lines and station details in Wanninkhof et al., 2014).

S3. Silica to Nutrient Limitation Ratios

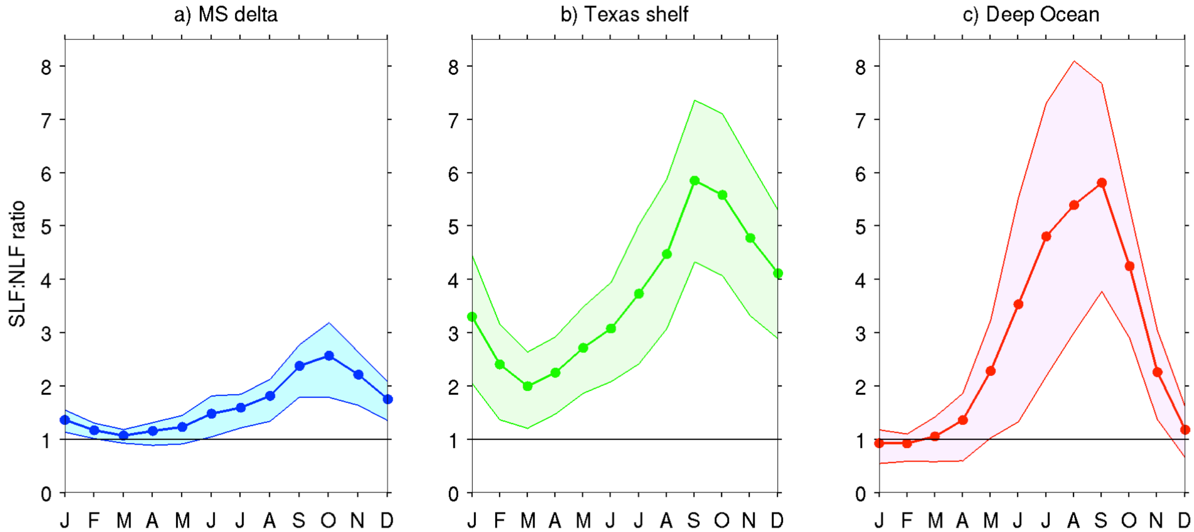

Figure S10. Climatological patterns of the ratio of silica to nitrogen limitation (SLF:NLF) in the Mississippi delta, Texas shelf, and Deep Ocean regions (depicted in Fig. 1). Coloured areas represent the interquartile range derived from monthly model outputs. SLF:NLF < 1 implies diatom's growth limitation is due to silica.

S4. Fennel-GoMBio chlorophyll comparison

Comparison between Fennel and GoMBio chlorophyll patterns

We coupled our ocean circulation model to the 7-component Fennel's biogeochemical model -using same parameter values as Fennel et al. (2011)- to evaluate in what degree the derived Fennel's chlorophyll patterns differ from the ones derived from GoMBio. The comparison reveals important differences in terms of the model ability to reproduce the chlorophyll patterns in the coastal and oceanic regions. In the Mississippi delta and Texas shelf, the correlation between Fennel's chlorophyll and SeaWiFS is similar to that between GoMBio and SeaWiFS, but Fennel's model does better than GoMBio reproducing the mean satellite condition. On the other hand, GoMBio reproduces better than Fennel the temporal variability and long-term mean of satellite chlorophyll in the Deep Ocean, not showing the chlorophyll seasonal bias observed in Fennel's model during winter (Fig. S11c and S12). It is worth to note that the winter chlorophyll overestimation in Fennel's model is consistent with results by Xue et al. (2013) (see their Figure 8).

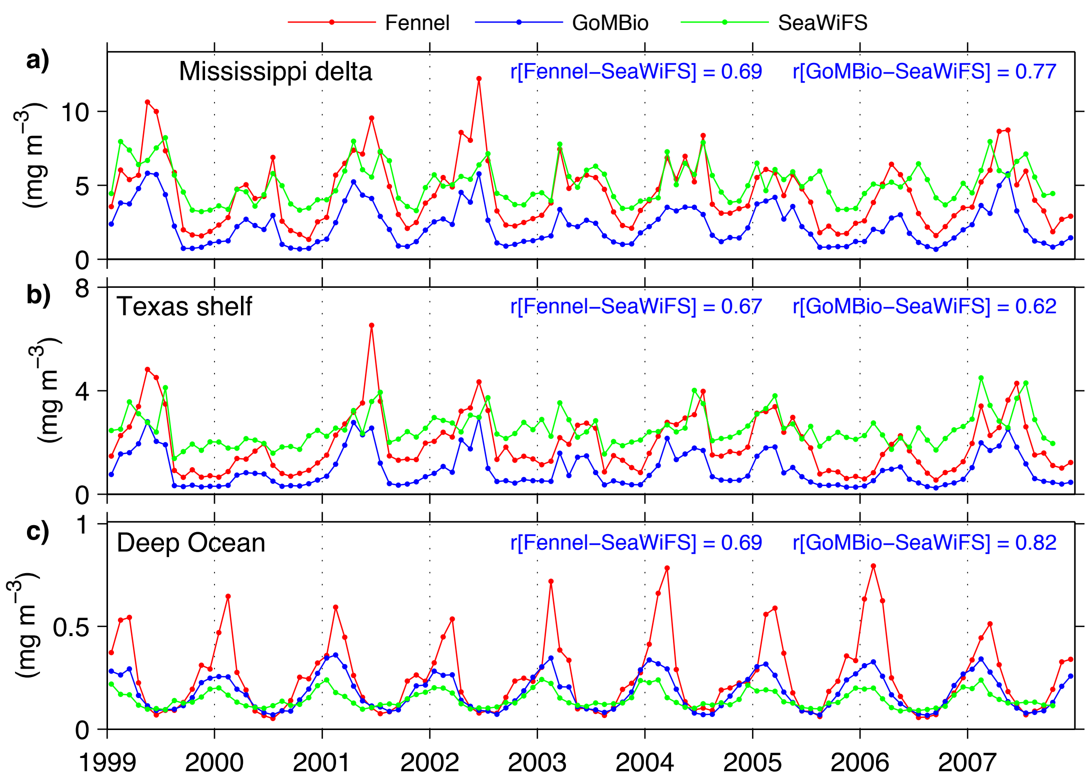

Figure S11: Surface chlorophyll series derived from Fennel (red) and GoMBio (blue) biogeochemical models, and SeaWiFS (green). Correlation coefficient between the modeled and SeaWiFS time series is indicated at each panel.

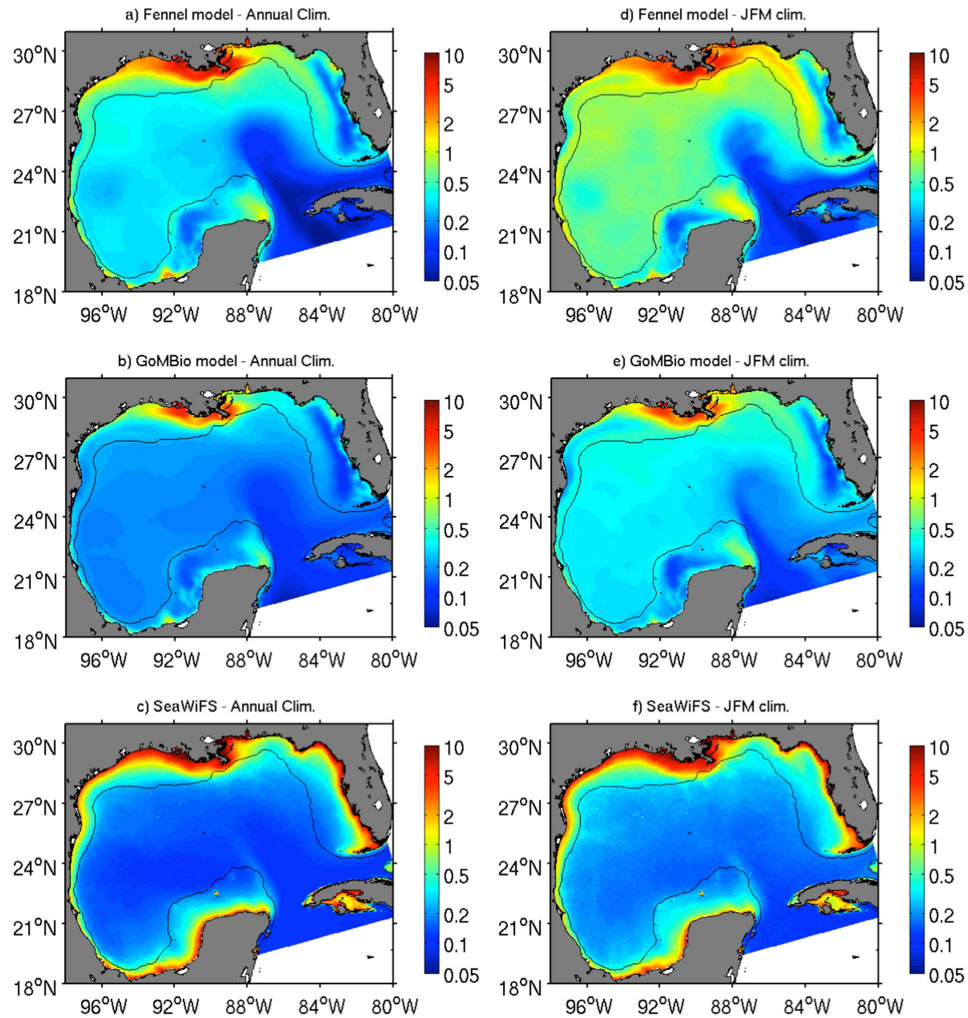

Figure S12. Surface chlorophyll climatology derived from a) Fennel model, b) GoMBio model and c) SeaWiFS during 1999-2005. d-f) as in a-c but for Jan-March only.

Model sensitivity to zooplankton grazing parameters

The winter chlorophyll overestimation derived from Fennel's model in the Deep Ocean might be linked to misrepresentation of zooplankton grazing, as Fennel's model does not explicitly simulate microzooplankton. This could lead to grazing underestimation in regions where the mean phytoplankton biomass is small, like in the deep Gulf. Here we perform two simple sensitivity experiments to evaluate whether the inclusion of two zooplankton types help to produce more realistic chlorophyll patterns in the Deep Ocean region. In the first sensitivity experiment (EXP-Z1), the biogeochemical model includes only one zooplankton type, which has a half-saturation constant of 0.50 (mmol m^{-3}) ^{2} and a maximum grazing rate of 0.16 day^{-1}, representing a parameterization in between micro- and mesozooplankton. In the second experiment (EXP-Z2), the biogeochemical model has the two zooplankton types (micro- and mesozooplankton), but the microzooplankton half-saturation constant (K_{ZS}) was increased to 0.9 (mmol m^{-3}) ^{2}. In other words, we use same half saturation constant for micro- and mesozooplankton, which implies a slower microzooplankton response to the seasonal phytoplankton bloom. The results show that EXP-Z1 produces a greater chlorophyll peak than GoMBio but smaller than Fennel, while EXP-Z2 closely match the winter chlorophyll peak obtained with Fennel's model (Fig. S13), suggesting that the explicit representation of microzooplankton grazing with a small half-saturation constant can be relevant to constrain the amplitude of the winter chlorophyll peak.

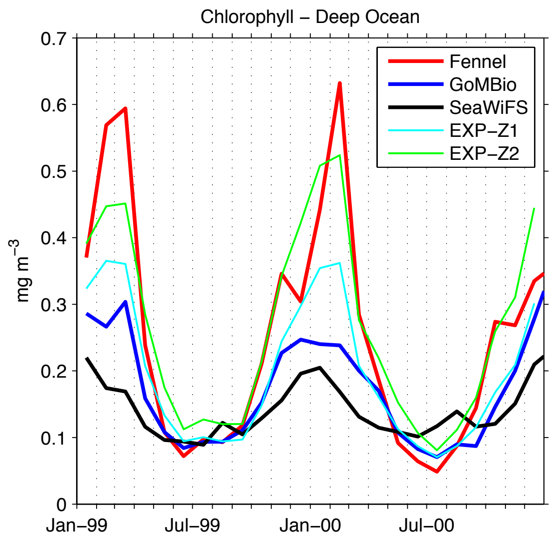

Figure S13: Sensitivity of chlorophyll to zooplankton grazing pressure in the Deep Ocean. Time series of surface chlorophyll in the Deep Ocean region derived from Fennel model (red), our 13-component model (blue), the model experiments zooplankton1 (cyan) and zooplankton2 (green), and SeaWiFS (black).